Quantitative analysis of the self-absorption and reemission effects on the emission spectrum of photoluminescence in right-angle excitation–detection configuration*

Wang Zhen-Hua(王振华), Wu Yu-E(吴玉娥), Zhang Xin-Zheng(张心正)†,
Yun Zhi-Qiang(云志强), Li Wei(李 威), and Xu Jing-Jun(许京军)

The Key Laboratory of Weak-Light Nonlinear Photonics, Ministry of Education, TEDA Applied Physics School and School of Physics, Nankai University, Tianjin 300457, *China*

(Received 27 February 2013; revised manuscript received 9 June 2013)

A theoretical approach based on differential radiative transport is proposed to quantitatively analyze the self-absorption and reemission effects on the emission spectrum for right angle excitation–detection photoluminescence measurements, and the wavelength dependence of the reemission effect is taken into account. Simulations and experiments are performed using rhodamine 6G solutions in ethanol as model samples. It is shown that the self-absorption effect is the dominant effect on the detected spectrum by inducing pseudo red-shift and reducing total intensity; whereas the reemission effect partly compensates for signal decrease and also results in an apparent signal gain at the wavelengths without absorption. Both effects decrease with the decrease in the sample concentration and the propagation distance of the emission light inside the sample. We therefore suggest that diluted solutions are required for accurate photoluminescence spectrum measurements and photoluminescence-based measurements.

Keywords: photoluminescence, self-absorption effect, reemission effect, radiative transport

PACS: 33.70.Jg, 33.50.Dq **DOI:** 10.1088/1674-1056/22/11/113301

1. Introduction

Photoluminescence (PL) is one of the most popular and powerful metrological tools in investigating light excited energy transition and transfer between atomic/molecular energy levels and related nonlinear optical properties of atoms and molecules, wherein the fluorescence lifetime and emission spectrum are sensitive to the variation of molecule configurations and the interaction with surrounding molecules.[1–6] However, for the specimen whose absorption and emission spectra overlap, the self-absorption of emission photons (radiation trapping) and subsequent reemission may induce significant measurement artifacts especially for dense solutions, which might result in mistakes in qualitative/quantitative analysis based on these measurements. Kühn *et al.*[7,8] suggested a pinhole method to minimize the self-absorption effect on the emission spectrum and lifetime by limiting the excitation and emission region in a solid specimen. In addition, the extraction of the excitation spectrum in the right-angle excitation–detection PL geometry was reported,[9] where only the self-absorption effect was considered. Cormier *et al.*[10] discussed both self-absorption and reemission effects on both the emission spectrum and lifetime for the same case, but in their theoretical model, the reemitted light from absorbed primary emission was assumed to be independent of wavelength and a constant reemission fraction was used for all emission wavelengths. This is an oversimplification for general conditions, and thus only the self-absorption effect showed up in their final theoretical results.

In this paper, we make a more detailed analysis of the self-absorption and reemission effects on the emission spectrum for the general right-angle excitation–detection PL as reported in Refs. [9] and [10]. A complete derivation of the differential evolution of the emission light intensity during its propagation in the PL sample is deduced, involving the wavelength-dependent self-absorption and reemission effects. Both theoretical simulations and experiments are performed using rhodamine 6G (Rh6G) solutions in ethanol as model samples. We show how the PL emission spectrum, including the signal intensity and peak position, is influenced by the self-absorption effect solely or together with the reemission effect. The article is organized as follows. The general theoretical derivations are presented in Section 2, the PL experimental setup and samples are described in Section 3, and both the theoretical simulation and experimental results are discussed in Section 4. The results are summarized in Section 5.

2. Theoretical approach

The theoretical model is based on the radiative transport of exciting/emission light in a general right-angle excitation–detection configuration for PL measurements as shown in

*Project supported by the National Basic Research Program of China (Grant No. 2010CB934101), the National Natural Science Foundation of China (Grant No. 11174161), and the International S&T Cooperation Program of China (Grant No. 2011DFA52870).

†Corresponding author. E-mail: zxz@nankai.edu.cn

© 2013 Chinese Physical Society and IOP Publishing Ltd

Fig. 1. An excitation beam illuminates the sample from one side of the cuvette. Assuming the beam propagates along the x direction with a Gaussian profile in the y direction and constant in the z direction, we have

$$I_{\lambda_{ex}}(x,y) = I_0 \exp(-\alpha_{\lambda_{ex}} x) \cdot \exp[-2(y-w)^2/w^2], \quad (1)$$

where $\alpha_{\lambda_{ex}}$ is the absorption coefficient of the sample at excitation wavelength λ_{ex}, w is the half width at $1/e^2$ intensity along the y direction, and the two boundaries are assumed to be at $y_a = 0$ and $y_b = 2w$, respectively. The beam width is considered not to depend on x in the cuvette, for simplicity. The emission light perpendicular to the excitation beam in a small area at far-field is detected, which is considered to be the fraction of the emission along the y direction between X and $X+d$ only. In general, the excitation intensity in PL is relatively weak so that only the ground state absorption and the first excited state emission occur. Thus, the local emission spectrum is the intrinsic emission spectrum independent of excitation conditions. Hence, the region of interest is approximately the rectangle bounded by X and $X+d$ in the x direction and y_a and y_c in the y direction, where y_c is the position of the cuvette wall. To calculate the detected emission spectrum, we divide the valid region into volumes with and without excitation beams, and then divide each volume into small subvolumes of $\Delta x \times \Delta y$, as done in Ref. [9], as shown in the insert of Fig. 1.

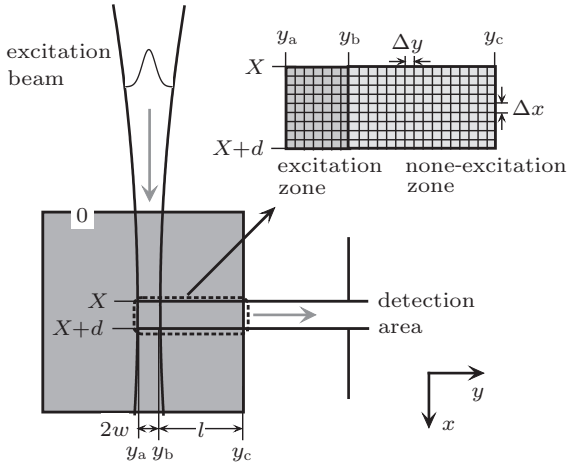


Fig. 1. Diagram of light propagation in the sample cuvette in a photoluminescence spectrometer with right-angle excitation–detection configuration.

2.1. Intrinsic emission spectrum

The local emission to the right angle from a subvolume (x, y) in the excitation zone is

$$\begin{aligned} I_{\lambda_{em}}(x,y)\Delta x\Delta y &= k_1 q e_{\lambda_{em}}(\lambda_{ex}/\lambda_{em}) I_{\lambda_{ex}}(x,y) \\ &\quad \times \Delta y[1-\exp(-\alpha_{\lambda_{ex}}\Delta x)] \\ &\approx k_1 \alpha_{\lambda_{ex}} q e_{\lambda_{em}}(\lambda_{ex}/\lambda_{em}) I_{\lambda_{ex}}(x,y)\Delta x\Delta y, \quad (2) \end{aligned}$$

where k_1 is the angle distribution coefficient of spontaneous emission at 90°; $qe_{\lambda_{em}}$ is the intrinsic differential quantum yield (QY) at emission wavelength λ_{em} of the sample; the factor $\lambda_{ex}/\lambda_{em}$ is introduced to transform photon numbers to light energy according to the definition of QY.[11,12] The approximation in Eq. (2) is accurate for $\alpha_{\lambda_{ex}}\Delta x \ll 1$.

If self-absorption and related effects are ignored, the detected signal $S_{\lambda_{em}}$ is described by the integral of the local emission intensity in Eq. (2) over the excitation zone multiplied by the detection efficiency C. Thus,

$$S_{\lambda_{em}} = C\int_X^{X+d}\int_{y_a}^{y_b} I_{\lambda_{em}}(x,y)\,\mathrm{d}x\mathrm{d}y. \quad (3)$$

Substituting Eqs. (1) and (2) into Eq. (3), we obtain

$$\begin{aligned} S_{\lambda_{em}}(X) &= C k_1 q e_{\lambda_{em}} \alpha_{\lambda_{em}} I_0 \lambda_{ex}/\lambda_{em} \\ &\quad \times \int_X^{X+d}\int_0^{2w} \exp(-\alpha_{\lambda_{em}} x) \\ &\quad \times \exp\left[\frac{-2(y-w)^2}{w^2}\right]\mathrm{d}x\mathrm{d}y \\ &= C k_1 \alpha_{\lambda_{em}} I_0 q e(\lambda_{ex}/\lambda_{em}) K_x Y, \quad (4) \end{aligned}$$

where $K_x = \exp(-\alpha_{\lambda_{ex}} X)[1-\exp(-\alpha_{\lambda_{ex}} d)]$ and $Y = (\pi)\mathrm{Erf}(\sqrt{2})w \approx 1.196w$ represent the contributions to the integral with respect to x and y, respectively. Here, the Erf function is the error function resulting from the finite integral of a Gaussian function, which is defined as

$$\mathrm{Erf}(z) = \frac{2}{\sqrt{\pi}}\int_0^z \exp(-t^2)\,\mathrm{d}t. \quad (5)$$

From Eq. (4) we can see that although the detected emission signal depends on the excitation conditions (λ_{ex}, $\alpha_{\lambda_{ex}}$, $I_{\lambda_{ex}}$) and the detection position X, these factors make equal contributions at all emission wavelengths. Thus, the detected emission spectrum (profile) is identical to the intrinsic emission spectrum, i.e., proportional to $qe_{\lambda_{em}}/\lambda_{em}$.

2.2. Emission spectrum only with self-absorption effect

The self-absorption effect occurs in the sample whose absorption and emission spectra partially overlap, and different emission wavelengths undergo different processes of absorption when propagating in the sample. One approach to describe this effect is by calculating the discrete power arriving at the boundary y_b by multiplying the local emission power (Eq. (2)) with the corresponding transmission factor at λ_{em} for each subvolume,

$$I'_{\lambda_{em}}(x,y)\Delta x\Delta y = I_{\lambda_{em}}(x,y)\Delta x\Delta y \exp[-\alpha_{\lambda_{em}}(y_b - y)], \quad (6)$$

where $\alpha_{\lambda_{em}}$ is the absorption coefficient at λ_{em}. Then, the total emission power $E'_{\lambda_{em}}$ at y_b is obtained by the integral over the excitation zone as

$$\begin{aligned} E'_{\lambda_{em}}(X, y_b) &= \int_X^{X+d}\int_{y_a}^{y_b} I'_{\lambda_{em}}(x,y)\,\mathrm{d}x\mathrm{d}y \\ &= k_1 \alpha_{\lambda_{ex}} I_0 q e_{\lambda_{em}}(\lambda_{ex}/\lambda_{em}) K_x Y', \quad (7) \end{aligned}$$

where Y' is the y direction contribution to the integral, i.e.,

$$Y' = \frac{1}{2}\sqrt{\frac{\pi}{2}}w\exp\left(-\alpha_{\lambda\mathrm{em}}w+\frac{\alpha_{\lambda\mathrm{em}}^2w^2}{8}\right) \times\left[\mathrm{Erf}\left(\frac{4w+\alpha_{\lambda\mathrm{em}}w^2}{2\sqrt{2}w}\right)-\mathrm{Erf}\left(\frac{-4w+\alpha_{\lambda\mathrm{em}}w^2}{2\sqrt{2}w}\right)\right]. \quad (8)$$

Since the power evolution in the non-excitation zone is governed only by the absorption process of the total emission power $E'_{\lambda\mathrm{em}}$, the detected signal out of the cuvette should be

$$\begin{aligned} & S'_{\lambda\mathrm{em}}(X,y_\mathrm{c}) \\ &= CE'_{\lambda\mathrm{em}}(X,y_\mathrm{b})\exp(-\alpha_{\lambda\mathrm{em}}l) \\ &= Ck_1\alpha_{\lambda\mathrm{ex}}I_0qe_{\lambda\mathrm{em}}(\lambda_{\mathrm{ex}}/\lambda_{\mathrm{em}})K_xY'\exp(-\alpha_{\lambda\mathrm{em}}l), \end{aligned} \quad (9)$$

where $l = y_\mathrm{c} - y_\mathrm{b}$, as shown in Fig. 1.

Alternatively, this effect can be described by a discrete analysis of the evolution of total emission power along the y axis. Since the emission power arriving at $y_1 = \Delta y$ from the first discrete subvolume denoted by (x, y_1) is proportional to the local excitation intensity, we have

$$E'_{\lambda\mathrm{em}}(x,y_1) = QI_{\lambda\mathrm{ex}}(x,y_1), \quad (10)$$

where $Q = k_1\alpha_{\lambda\mathrm{ex}}qe_{\lambda\mathrm{em}}(\lambda_{\mathrm{ex}}/\lambda_{\mathrm{em}})\Delta x\Delta y$. While the total emission power arriving at $y_2 = 2\Delta y$ is the sum of the local excitation in subvolume (x, y_2), $E'_{\lambda\mathrm{em}}(x, y_1)$ which experiences absorption loss can be described by

$$E'_{\lambda\mathrm{em}}(x,y_2) = QI_{\lambda\mathrm{ex}}(x,y_2)+E'_{\lambda\mathrm{em}}(x,y_1)\exp(-a_{\lambda\mathrm{em}}\Delta y). \quad (11)$$

Similarly, the total emission power arriving at y_n is

$$\begin{aligned} E'_{\lambda\mathrm{em}}(x,y_n) &= QI_{\lambda\mathrm{ex}}(x,y_n)+E'_{\lambda\mathrm{em}}(x,y_{n-1}) \\ &\quad\times\exp(-a_{\lambda\mathrm{em}}\Delta y), \end{aligned} \quad (12)$$

where $n = 2,3,\ldots$. Repeating the power evolution until the boundary $y_\mathrm{b} = y_N = N\Delta y$ is approached, we obtain

$$\begin{aligned} E'_{\lambda\mathrm{em}}(x,y_N) &= QI_{\lambda\mathrm{ex}}(x,y_N)+E'_{\lambda\mathrm{em}}(x,y_{N-1})\exp(-a_{\lambda\mathrm{em}}\Delta y) \\ &= Q\sum_{i=1}^{N}I_{\lambda\mathrm{ex}}(x,y_i)\exp[-\alpha_{\lambda\mathrm{em}}(N-i)\Delta y]. \end{aligned} \quad (13)$$

For $\alpha_{\lambda\mathrm{em}}\Delta y \ll 1$, the integral of Eq. (13) along the x axis is equal to Eq. (7). Therefore, the power evolution in the non-excitation zone is again described by absorption only and the final detected signal is equal to Eq. (9). Actually, this result is equivalent to the result in Ref. [9] except that a more realistic Gaussian profile of the excitation beam is considered here.

Since the emission power evolution is independent of x, the integral along the x axis does not influence the detected emission spectrum, as in the non-self-absorption case, while the evolution along the y axis will substantially change the measured spectrum due to absorption dispersion. In order to better describe the self-absorption effect, the expression $Y'\exp(-\alpha_{\lambda\mathrm{em}}l)$ in Eq. (9) should be divided out for each λ_{em}. However, if the width of the excitation beam is very small and $\alpha_{\lambda\mathrm{em}}w \ll 1$, the factor Y' is reduced into $Y' = \sqrt{\pi/2}\cdot\mathrm{Erf}(\sqrt{2})w = Y$, and only the transmission factor $\exp(-\alpha_{\lambda\mathrm{em}}l)$ is involved.

2.3. Emission spectrum with reemission effect

For the specimen with high fluorescence QYs, such as dye molecules, where both the self-absorption of emission photons and subsequent reemission cannot be ignored, things are more complicated. We analyze this situation using discrete analysis of the evolution of emission power along the $y$axis, as in the case of the self-absorption effect.

The emission power arriving at y_1 from subvolume (x, y_1) is again written as

$$E''_{\lambda\mathrm{em}}(x,y_1) = E'_{\lambda\mathrm{em}}(x,y_1) = QI_{\lambda\mathrm{ex}}(x,y_1). \quad (14)$$

The total emission power arriving at y_2 comes partly from the local excitation in subvolume (x, y_2), partly from $E'_{\lambda\mathrm{em}}(x, y_1)$ propagating to y_2 with absorption loss, and partly from the contribution of reemission excited by the absorbed part of $E'_{\lambda\mathrm{em}}(x, y_1)$. As a result,

$$\begin{aligned} E''_{\lambda\mathrm{em}}(x,y_2) &= QI_{\lambda\mathrm{ex}}(x,y_2)+E''_{\lambda\mathrm{em}}(x,y_1)\exp[-\alpha_{\lambda\mathrm{em}}\Delta y] \\ &\quad+\mathrm{Rm}_{\lambda\mathrm{em}}(x,y_1), \end{aligned} \quad (15)$$

where $\mathrm{Rm}_{\lambda\mathrm{em}}(x, y_i)$ represents the sum of reemission power at λ_{em} excited by the absorbed photons of previous emission at all λ'_{em} and can be expressed as

$$\begin{aligned} & \mathrm{Rm}_{\lambda\mathrm{em}}(x,y_i) \\ &= k_2\sum_{\lambda'_{\mathrm{em}}}E''_{\lambda\mathrm{em}'}(x,y_i)[1-\exp(-\alpha_{\lambda\mathrm{em}'}\Delta y)]\lambda'_{\mathrm{em}}qe_{\lambda\mathrm{em}}/\lambda_{\mathrm{em}} \\ &= (k_2qe_{\lambda\mathrm{em}}/\lambda_{\mathrm{em}})\sum_{\lambda'_{\mathrm{em}}}E''_{\lambda\mathrm{em}'}(x,y_i)a_{\lambda\mathrm{em}'}\Delta\mathrm{y}\lambda'_{\mathrm{em}}. \end{aligned} \quad (16)$$

Here $i = 1,2,\ldots$ and k_2 is the angle distribution coefficient of the PL emission parallel to the previous emission along the y axis, since only this fraction contributes to the detected signal.

Consequently, the total emission power evolves along the $y$axis in the excitation zone. Then, we have

$$\begin{aligned} E''_{\lambda\mathrm{em}}(x,y_n) &= QI_{\lambda\mathrm{ex}}(x,y_n)+E''_{\lambda\mathrm{em}}(x,y_{n-1})\exp[-\alpha_{\lambda\mathrm{em}}\Delta y] \\ &\quad+\mathrm{Rm}_{\lambda\mathrm{em}}(x,y_{n-1}), \end{aligned} \quad (17)$$

where $n = 2,3,\ldots,N$ and $y_N = y_\mathrm{b}$. The power evolution in the non-excitation zone is similar to that in the excitation zone, except that the local excitation term is missing. Thus,

$$E''_{\lambda\mathrm{em}}(x,y'_0) = E''_{\lambda\mathrm{em}}(x,y_\mathrm{b}), \quad (18)$$

$$\begin{aligned} E''_{\lambda\mathrm{em}}(x,y'_k) &= E''_{\lambda\mathrm{em}}(x,y'_{k-1})\exp[-\alpha_{\lambda\mathrm{em}}\Delta y] \\ &\quad+Rm_{\lambda\mathrm{em}}(x,y'_{k-1}), \end{aligned} \quad (19)$$

where $k = 1,2,\ldots,M$, and $y'_M = y_b + M\Delta y = y_c$. Finally, we obtain the detected signal as

$$S''_{\lambda em} = C\int_X^{X+d} E''_{\lambda em}(x, y_c). \tag{20}$$

From the derivation above, we can see that the emission energies at different wavelengths couple with each other via self-absorption and subsequent reemission effects along the y direction in both excitation and non-excitation zones. Since the reemission terms vary with the evolution of the emission power along the y axis in the sample, it is impossible to divide these artifacts analytically. Nevertheless, a revival program based on the above derivation might be produced to reconstruct a purified emission spectrum. Here, again the integral with respect to x could be extracted as K_x and have no contribution to the emission spectrum shift. Compared with our results, the assumption of a constant efficiency as a reemission factor in Ref. [10] was oversimplified. Thus, only the self-absorption effect actually plays a role on the profile of their emission spectrum $S_{\lambda em} = C_{\lambda ex}[1 - \alpha_{\lambda em}]E_{\lambda em}$ according to Eq. (11) in Ref. [10], where $C_{\lambda ex}$ is related only to the initial excitation wavelength and position.

3. Experimental setup and samples

To reveal the coupling of self-absorption and reemission effects on the emission spectrum, we carried out experiments using a fluorescence spectrometer (FSL920, Edinburgh Instrument Ltd.) in a general right-angle excitation–detection configuration, as shown in Fig. 2. Three provisions were introduced to make the experimental situation approach the theoretical model. (1) A slit (~ 4 mm in width) denoted as 'Slit 1' was put before Lens 1 ($f = 300$ mm) to confine the input beam width so that the excitation beam inside the sample has an approximately uniform width along the x direction. (According to the beam transform relationship using a lens, the beam width within confocal parameter b along its propagation is approximately uniform, where b is related to the focal length of the lens f, the light wavelength λ, and the input beam width D by $b \approx 8f^2\lambda/(\pi D^2)$, thus a long focal length and a narrow input beam width can result in a longer propagation distance with uniform beam width near the focus.) (2) Another slit 'Slit 2' was aligned before Lens 2 to confirm that most right-angle emissions from the region of interest were detected. (3) The sample holder was mounted on a two-dimensional translation stage, so that the sample position, especially the distance from the excitation beam to the lateral wall of the cuvette, could be varied. The resolution for both the excitation and emission bandwidths was fixed to be 1 nm for all experiments.

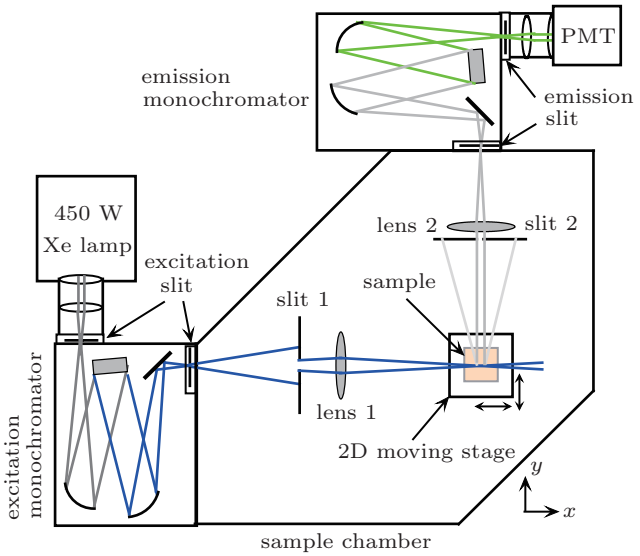


Fig. 2. (color online) Experimental setup to reveal self-absorption and reemission effects on emission spectrum.

The popular dye Rhodamine 6G (Rh6G) solutions in ethanol were chosen as model samples for both theoretical and experimental tests. Stock solution containing 0.001 mol/L (M) Rh6G (Sigma) was prepared with AR grade ethanol, and lower concentration solutions were obtained by dilution. Absorbencies were measured with a UV–visible spectrophotometer (U-4100, Hitachi) using cuvettes with 1 or 10 mm path length, depending on the concentration, which were used to verify the diluted concentrations according to the Beer–Lambert law and to the standard data of molar extinction efficiencies.[13,14] The emission spectrum of a 5×10^{-7} M solution excited at 480 nm was used to compute the differential QY $qe_{\lambda em}$ for theoretical calculations. (The measured intensity $I_{\lambda em}$ at each λ_{em} was first transferred to photon numbers by multiplying the corresponding λ_{em}. Then, the resulting data were renormalized to be $qe_{\lambda em}$ so that $\sum_{\lambda em} qe_{\lambda em} = QE$, where QE was the total QY and was taken as QE=0.95.[15]) The extinction efficiencies ε and $qe_{\lambda em}$ at the wavelengths of interest are shown in Fig. 3. Note that ε was set to be 0 for $\lambda > 700$ nm according to the standard data[13,14] and our measurements.

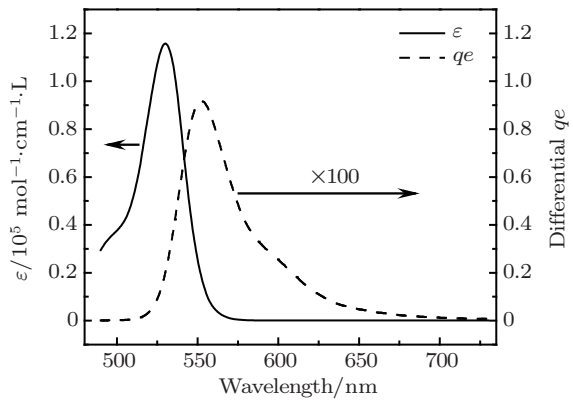


Fig. 3. Molar extinction efficiencies ε and differential quantum yields $qe_{\lambda em}$ at wavelengths of interest for an Rh6G solution in ethanol.

4. Results and discussion

4.1. Numerical simulations

In Figs. 4(a) and 4(b), the simulation results with and without the reemission effect are depicted. They refer to the theoretical derivation and a $c = 4 \times 10^{-4}$ M Rh6G solution. The black solid lines denoted as 'pure emission' in all pictures are the normalized intrinsic emission spectra without considering any artificial effects according to Eq. (4). As shown in Fig. 4(a), if only the self-absorption effect is taken into account, the detected intensity at the wavelengths where emission and absorption spectra overlap decreases exponentially with the propagation distance. Since the signals at shorter wavelengths drop much faster than those at longer wavelengths, due to absorption dispersion, a significant red-shift appears in the detected spectrum and increases with the propagation distance. Note that a finite width $(2w)$ of the excitation beam already induces a marked change in the detected emission spectrum, so excitation even close to the cuvette wall $(l = 0)$ could not eliminate the self-absorption effects.

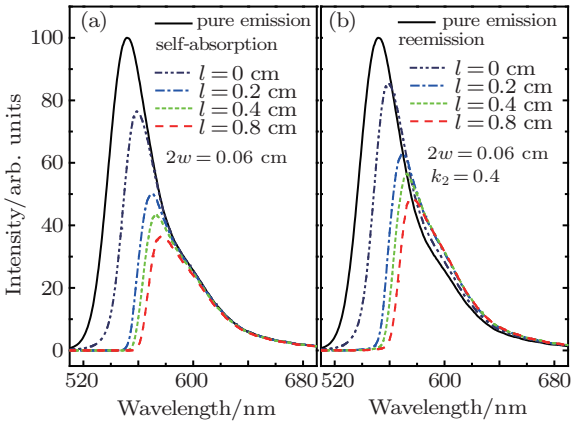


Fig. 4. (color online) Theoretical simulation of (a) only self-absorption effects and (b) together with reemission effects on emission spectrum for different propagation distances in a Rh6G solution with $c = 0.4$ mM.

An additional signal appears in the detected spectrum if the reemission effect is taken into account, as shown in Fig. 4(b). Here the angle distribution factor of reemission is set to $k_2 = 0.4$. The signal at shorter wavelengths exhibits a smaller but significant decrease with the propagation distance than in the pure self-absorption cases, which indicates the self-absorption effect is still the dominant effect on the change of detected emission spectrum. However, except for the red-shift artifact, there is a distinct increase in the emission signal at longer wavelengths. This indicates that the reemission effect partly compensates for the self-absorption effect at shorter wavelengths and also induces an over-compensated gain at longer wavelengths, and finally results in a complex change in the detected emission spectrum. Such a gain signal could not be expected without considering the wavelength-dependent reemission factor, as discussed in Ref. [10].

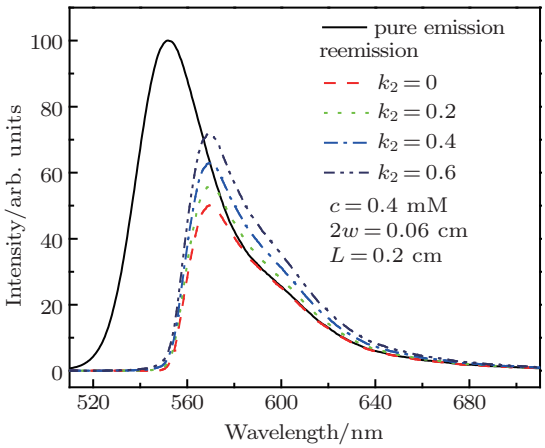


Fig. 5. (color online) Simulation of the influence of fluorescence quantum yields on emission spectrum, with the reemission effect considered by adjusting the angle distribution factor k_2 in Rh 6G solution for $l = 0.2$ cm and $c = 0.4$ mM.

Due to the nature of photoluminescence, the angle-distribution factor k_2 might be a fixed value related to the sample at a special direction. However, since it is involved in the reemission effect by multiplying with fluorescence QYs as in Eq. (17), the variation of k_2 could be considered as the change of QYs and is used to simulate the influence of QYs on the reemission effect, as shown in Fig. 5. It is evident that the reemission signal decreases with the decrease in QYs (here k_2), but the red-shift from the self-absorption effect remains unchanged. This indicates that the reemission effect, rather than the self-absorption effect, might be ignored for PL samples with very low quantum yields. This explains why only self-absorption was considered in Ref. [9] since their eumelanin sample has extremely low quantum yields.

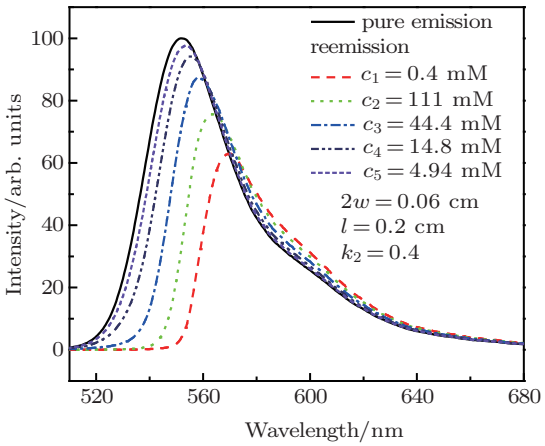


Fig. 6. (color online) Simulation of the influence of sample concentration on emission spectrum considering reemission effect in Rh6G solution for $l = 0.2$ cm and $k_2 = 0.4$.

The influence of concentration on the emission spectrum in view of the reemission effect is also studied, as shown in Fig. 6. Note that all spectra are normalized with its intrinsic emission (the pure emission) since the evolvement of excitation light is not taken into account in this paper. With the decrease in concentration, the absorption at all wavelengths de-

creases consequently, and thus the reemission excited by the absorbed light is reduced. Therefore, both the red-shift and the additional increment at longer wavelengths decrease with decreasing concentration. This indicates that the only way to minimize these two effects in experimental measurements is by diluting the sample for the present PL setup.

4.2. Experimental results

Experimental studies of the dependence of detected emission spectra on the propagation distance (l) were carried out using Rh6G solutions in ethanol with different concentrations. Typical spectra as compared with corresponding simulations in a $c = 3.84 \times 10^{-4}$ M solution are presented in Fig. 7. First, because exciting close to the lateral boundary of the cuvette ($l = 0.0$ cm) would suffer from scattering loss of the excitation intensity and result in a non-determinable decrease in the detected emission signal, we did not normalize the spectra with that for $l = 0.0$ cm. Hence, all the experimental results were normalized with the peak intensity of the spectrum for $l = 0.2$ cm. Second, the normalized simulation spectrum for $l = 0.2$ cm consistent with that of the experimental result was achieved by solely adjusting the parameter k_2, and the agreement was judged by the agreement of the peak positions on these two spectra. Then the following simulation with the same k_2 but with different l were plotted and compared with experimental results. As seen in Fig. 7, except for the result at $l = 0.0$ cm, the remaining spectra are quantitatively consistent with the theoretical simulations that considered reemission effect using $k_2 = 0.2$. This confirms that our theoretical model considering both the self-absorption and reemission effects agrees very well with the experimental results. $k_2 = 0.2$ indicates that reemission is a rather small but non-negligible effect with respect to emission spectrum measurements for high QY samples.

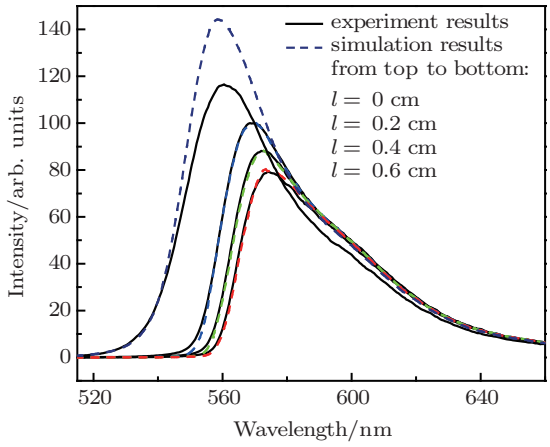


Fig. 7. (color online) Detected emission spectra (black solid lines) of Rh6G solution with $c = 3.84 \times 10^{-4}$ M for different propagation distances compared with theoretical simulation with $k_2 = 0.2$ (colored dashed lines).

Peak positions of experimental and simulated emission spectra in Rh6G solution with different concentrations are picked up as the measure of emission spectral red-shifts, as shown in Fig. 8. The parameters used in the simulations including $l = 0.4$ cm, $2w = 0.06$ cm and the corresponding concentrations are the same as in the experiments described before. The k_2 is set to be 0.2 here. Red-shifts of the experimental spectra decrease with decreasing sample concentrations and perfectly agree with that of the simulation results. Note that the deviation is mostly due to the finite sampling interval of the spectrum, which is 0.5 nm in both the experiments and simulations.

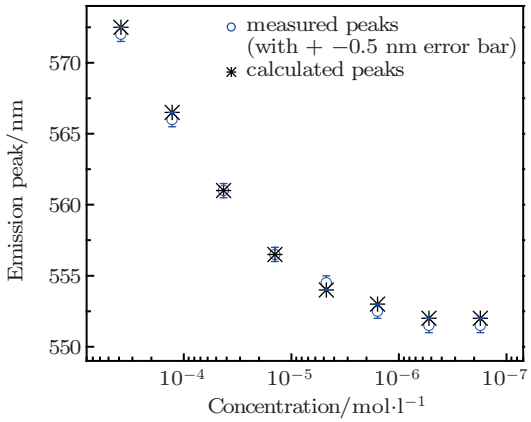


Fig. 8. (color online) Artificial spectral red-shifts of Rh6G solution with different concentrations.

5. Conclusion

In summary, theoretical models are proposed to quantitatively analyze the self-absorption and subsequent reemission effects on the detected emission spectrum in the general right-angle excitation–detection light-induced fluorescence configuration. Wavelength-dependent self-absorption and reemission effects are taken into account in the derivation of the differential evolution of the emission light intensity during its propagation in the PL specimen. Simulations use the data of Rh6G solutions in ethanol as model samples. Experiments were carried out using the same specimen with a commercial photoluminescence spectrometer. It is shown that self-absorption is the dominant effect on the detected emission spectrum which results in loss of the total signal and in a significant spectral red-shift artifact, while re-emission induces a generally small but distinct effect which partly compensated the self-absorption loss at the wavelengths where emission and absorption spectra overlap, and also led to signal gain at emission wavelengths without absorption. Both the self-absorption and reemission effects decrease with the decrease of the emission light propagation distance in the sample and the sample concentration. The reemission effect is positively related to the fluorescence quantum yields and can be ignored for the low quantum yields specimen, which could be analytically eliminated. Experimentally, diluted solutions are suggested to reduce the self-absorption and reemission artifacts in photoluminescence and

related spectral measurements. Based on our analysis, a reconstruction program might be employed to eliminate such artifacts. Note that all of the above discussions are not limited to liquid solutions but are also suitable for radiative molecules or atoms dispersed in polymers, gels, crystals, or glass.

Acknowledgment

We thank Peter Hertel for valuable advices.

References

[1] Petrov E P, Bogomolov V N, Kalosha I I and Gaponenko S V 1998 *Phys. Rev. Lett.* **81** 77
[2] Xia Z and Liu Y 2001 *Biophys. J.* **81** 2395
[3] Becker K, Lupton J M, Feldmann J, Nehls B S, Galbrecht F, Gao D and Scherf U 2006 *Adv. Funct. Mater.* **16** 364
[4] Sakuma K, Hirosaki N and Xie R J 2007 *J. Lumin.* **126** 843
[5] Heikenfeld J, Garter M, Lee D S, Birkhahn R and Steckl A J 1999 *Appl. Phys. Lett.* **75** 1189
[6] Li X P, Chen B J, Shen R S, Zhang J S, Sun J S, Cheng L H, Zhong H Y, Tian Y, Fu S B and Du G T 2013 *Chin. Phys. B* **22** 023202
[7] Kühn H, Petermann K and Huber G 2010 *Opt. Lett.* **35** 1524
[8] Kühn H, Fredrich-Thornton S T, Kränkel C, Peters R and Petermann K 2007 *Opt. Lett.* **32** 1908
[9] Nighswander-Rempel S P, Riesz J, Gilmore J, Bothma J P and Meredith P 2005 *J. Phys. Chem. B* **109** 20629
[10] Cormier J F, Fortin M, Fréchette J, Noiseux I, Vernon M L and Long W 2005 *Proc. SPIE* **5702** 123
[11] Gaigalas K and Wang L L 2008 *J. Res. Natl. Inst. Stand. Technol.* **113** 17
[12] Suzuki K, Kobayashi A, Kaneko S, Takehira K, Yoshihara T, Ishida H, Shiina Y, Oishi S and Tobita S 2009 *Phys. Chem. Chem. Phys.* **11** 9850
[13] Du H, Fuh R A, Li J, Corkan L A and Lindsey J S 1998 *Photochem. Photobiol.* **68** 141
[14] Prahl S *Optical Absorption and Emission Data of Rhodamine 6G*
[15] Magde D, Wong R and Seybold P G 2002 *Photochem. Photobiol.* **75** 327